Engineering Failure Analysis 80 (2017) 241–252

Contents lists available at ScienceDirect

Engineering Failure Analysis

journal homepage: www.elsevier.com/locate/engfailanal

Mechanical failure mechanisms and forms of normal and deformed coal combination containing gas: Model development and analysis

Shouqing Lu[a,b], Lei Li[a], Yuanping Cheng[c,*], Zhanyou Sa[a], Yongliang Zhang[a], Ning Yang[a]

[a] Department of Safety Engineering, Qingdao Technological University, Qingdao, China
[b] State Key Laboratory Cultivation Base for Gas Geology and Gas Control (Henan Polytechnic University), Jiaozuo, China
[c] National Engineering Research Center of Coal Gas Control, China University of Mining & Technology, Xuzhou, China

ARTICLE INFO

Keywords:
Coal combination
Failure mechanisms
Coal mining
Coal and gas outburst

ABSTRACT

In coal mining, coal seams often contain several normal coal layers and deformed coal layers in the same region. However, the existence of deformed coal may promote the occurrence of coal and gas outbursts. To analyze the role of failure of different combinations of deformed coal on coal and gas outbursts, force analysis of normal and deformed coal combinations containing gas was carried out, and the expressions of interfacial stress induced by uncoordinated horizontal deformation were first derived in this paper. The results showed that the additional interfacial stresses are affected by the external stresses, internal gas pressure, gas sorption-induced swelling deformation and mechanical parameters of coal and that the additional interfacial stresses on the normal coal and deformed coal are equal and opposite. Then, based on the Mohr-Coulomb criterion and uncoordinated deformation, the mechanical failure mechanisms and forms of combinations containing gas under ideal conditions were analyzed. We found that there are seven failure forms for the combination containing gas, and in most cases, the destruction of the combination is caused by the structural failure of deformed coal. Finally, the failure mechanisms of the combination due to mining were discussed using the parameters from the Qinshui Basin. The results showed that failure is more probable at the interface between the deformed coal and normal coal bodies and that the existence of deformed coal can promote the damage of normal coal. These research results can help us to better understand the role of mechanical failure in coal and gas outbursts within combinations, and provide a theoretical basis for the control of coal and gas outbursts.

1. Introduction

China boasts the largest number, scale and losses of coal and gas outburst disasters worldwide [1,2]. To meet the needs of economic growth, large quantities of coal must mined in the future [3], which will result in an increase in the mining depth of coal and more severe gas outburst disasters. Although the processes surrounding coal and gas outburst disasters are very complex, they occur under conditions requiring a certain amount of deformed coal in the regions of coal and gas outbursts [4–6]. Because of tectonic movement of the coal seam under the ground, intense plastic deformation may occur in some areas [7] and may form deformed coal layers. Deformed coal layers do not exist in isolation, and there are often several normal coal layers and deformed coal layers in the same place.

* Corresponding author at: National Engineering Research Center of Coal Gas Control, China University of Mining & Technology, Xuzhou, China.
E-mail address: Lusqcumt@cumt.edu.cn (Y. Cheng).

http://dx.doi.org/10.1016/j.engfailanal.2017.06.022
Received 27 March 2017; Received in revised form 6 June 2017; Accepted 14 June 2017
Available online 20 June 2017

After mining, the stress environment of coal and rock will be changed [8], which causes the coal to be damaged and even leads to coal and gas outbursts; thus, the failure of coal is the primary prerequisite for coal and gas outbursts. In a combination of normal and deformed coal, the strength of deformed coal is far less than that of normal coal; thus, deformed coal is the weak link of such a coal combination [9]. Moreover, deformed coal accelerates the development of failure of the combination and can even cause gas outburst disasters to occur. Beginning in the 1980s, scholars [10] found that the deformation and failure of this combination are affected by the adjoining rock or coal due to their different mechanical parameters. Depending on the different materials of the combination, they can be divided into rock-rock combinations, coal-rock combinations and coal-coal combinations.

Among the three types of combinations, rock-rock combinations were the first to be researched. Duffault [10] conducted research on the theory and numerical simulation of rock-rock combinations. Experimentally, Tziallas et al. [11] carried out mechanical experiments on mudstone and sandstone combinations with different proportions under uniaxial and triaxial stress states, and an empirical formula for predicting the compressive strength of combinations based on experimental data was obtained. From a theoretical perspective, Xian et al. [12] established a theoretical model of isotropic rock combinations and discussed the influence of parameters on the mechanical strength of combinations under different stress states. Li et al. [13] calculated the interfacial stress and analyzed the mechanical failure modes of rock-rock combinations under a uniaxial stress state.

Rocks can influence the deformation and failure of other rocks. Additionally, there are interaction effects between coal and rock owing to the lower mechanical strength of coal. The study of coal and rock combinations can help us to better understand the mechanisms of rock outbursts. Dou et al. [14] obtained the electromagnetic emission rule of coal and rock combinations during the loading process, the results of which were applied to the prediction of rock outbursts. To better understand the failure mechanisms of coal and rock combinations, a series of methods, including theoretical analysis, laboratory tests and numerical simulations, were used. The failure mechanisms of coal and rock combinations are governed by both external and internal influence factors [15]. The external factors mainly refer to the stress states of the combinations, while the external factors primarily refer to the properties of the combinations. Zuo et al. [16] found that splitting was the main failure form for combinations under a uniaxial stress state, while shear was the main failure form under a tri-axial stress state. In addition, the effects of rock strength, combined manners and inclined angles of combination on the failure mechanisms were researched by some scholars [17–19]. Based on the strain energy equivalency principle, Zhao et al. [20] established an analytical model for the failure criterion of combinations and discussed the failure forms of combinations that are affected by the interface strength, rock thickness and stress state.

Previously, greater effort was made to study rock-rock combinations or rock-coal combinations, and research regarding the failure mechanisms of coal-coal combinations was scarce. Using the simulation method, Li and Tan [21] analyzed the effects of the position of deformed coal on the failure of a combination, and they found that the intensity of coal and gas outbursts would be much stronger when the deformed coal constitutes the middle of the combination. Duan et al. [22] found that with the increase of the thickness of the deformed coal of the combination, the scale of a coal and gas outburst disaster would increase. Because the existence of deformed coal can make coal and gas outbursts much more probable [23,24], it is necessary to undertake a more comprehensive survey of the mechanical failure mechanisms of normal and deformed coal combinations containing gas, which can help to better understand the role of mechanical failure in coal and gas outbursts and to provide a theoretical basis for the control of coal and gas outbursts.

There is always a certain magnitude of interface cohesion between underground coal and rock [25]; therefore, this study was conducted based on the assumption that an interface cohesion between normal coal and deformed coal exists. In this paper, the uncoordinated horizontal deformation was first defined and deduced, and the interfacial stress expressions were obtained. Then, the mechanical failure mechanisms and forms of combinations containing gas under ideal conditions were analyzed, and seven failure forms for normal and deformed coal combinations containing gas were found. Finally, the failure mechanisms of normal and deformed coal combinations due to mining were discussed using parameters from the Qinshui Basin.

2. Force analysis

2.1. Force analysis of normal and deformed coal bodies

Normal coal and deformed coal are both assumed to exist within a homogeneous and isotropic medium, and the two coals are closely connected to one another between the layers. Before destruction, the two coals are regarded as one body during analyses of the stress state and the deformation of the combination. Biot's coefficient of coal is deemed to be 1. As shown in Fig. 1, the coal combination is affected by the external stresses in three directions, the internal gas pressure and the gas sorption-induced swelling deformation.

In this paper, the coal body is defined as the coal far away from the interface, and the coal interface is defined as the coal closest to the interface. For the coal bodies far away from the interfaces, their deformation cannot be affected by the deformation of other coals; thus, they can maintain their respective characteristics of deformation similar to a single coal body. The force conditions of normal and deformed coal bodies far away from the interfaces are the same, and the stress expressions can be expressed as:

$$\begin{cases} \sigma_{1n} = \sigma_{1d} = \sigma_1 - p \\ \sigma_{2n} = \sigma_{2d} = \sigma_2 - p \\ \sigma_{3n} = \sigma_{3d} = \sigma_3 - p \end{cases} \tag{1}$$

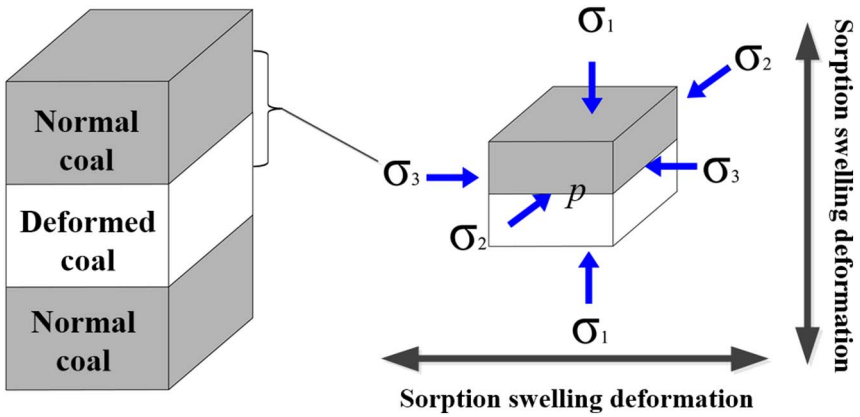

Fig. 1. Force analysis of a normal and deformed coal combination.

2.2. Force analysis of normal and deformed coal interfaces

For a combination of normal and deformed coal, the vertical deformations of normal coal and deformed coal cannot influence each other; therefore, the vertical effective stresses of normal and deformed coal interfaces are the same as those of their bodies. The value of the vertical effective stress is equivalent to the vertical effective stress minus the gas pressure, and the value of the horizontal effective stress is equal to the horizontal effective stress minus the gas pressure. In addition to the impact of the horizontal effective stress, the interfaces are affected by the additional stresses induced by uncoordinated horizontal deformation. The additional stresses on the normal coal and deformed coal are equal and opposite. The additional interfacial stresses are caused by uncoordinated horizontal deformation; thus, all of the factors that affect the uncoordinated horizontal deformation can affect the values of the additional interfacial stresses, including the external stresses, internal gas pressure, gas sorption-induced swelling deformation and mechanical parameters of coal.

When normal coal and deformed coal are separated, the relationship between the horizontal deformations of the two coals under the comprehensive action of stresses, gas pressure and swelling deformation can be divided into three situations. First, the horizontal deformation of normal coal is less than that of deformed coal. When the normal coal and deformed coal are regarded as a combination, the additional stresses place the normal coal interface in compression and the deformed coal interface in tension, as is shown in Fig. 2 (*a*). Second, the horizontal deformation of normal coal is equal to that of deformed coal, wherein there are no additional stresses at the interfaces, as shown in Fig. 2 (*b*). Finally, the horizontal deformation of normal coal is greater than that of deformed coal. When the normal coal and deformed coal are regarded as a combination, the additional stresses place the normal coal interface in tension and the deformed coal interface in compression, as shown in Fig. 2 (*c*). Force analysis of normal and deformed coal interfaces is shown in Fig. 2.

In this paper, analyses of the deformation and force along the interfaces are based on the situation illustrated in Fig. 2 (*a*). There are additional stresses at the interfaces due to the uncoordinated horizontal deformation, and the horizontal deformation of normal coal is equal to that acting on the deformed coal before destruction. Combined with the continuous deformation condition and static balance equations, we can obtain the following:

$$\begin{cases} \sigma_{1jn} = \sigma_1 - p \\ \sigma_{2jn} = \sigma_2 - p + \Delta_2 \\ \sigma_{3jn} = \sigma_3 - p + \Delta_3 \end{cases} \tag{2}$$

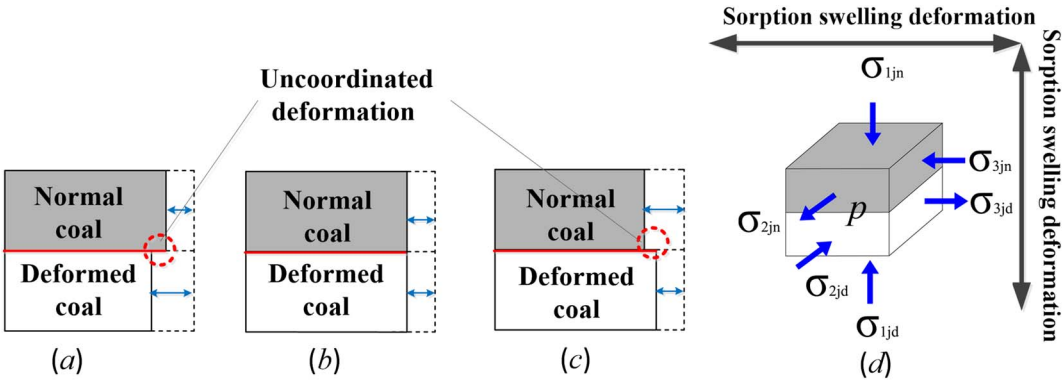

Fig. 2. Force analysis of normal and deformed coal interfaces.

$$\begin{cases}\sigma_{1jd} = \sigma_1 - p \\ \sigma_{2jd} = \sigma_2 - p - \Delta_2 \\ \sigma_{3jd} = \sigma_3 - p - \Delta_3 \end{cases} \tag{3}$$

$$\begin{cases}\varepsilon_{2jn} = \varepsilon_{2jd} \\ \varepsilon_{3jn} = \varepsilon_{3jd} \end{cases} \tag{4}$$

According to Hooke's Law and the constitutive relationship of coal, the relationships of stress and strain in the horizontal direction for the normal and deformed coal combination containing gas can be expressed as follows (positive in compression):

$$\begin{cases}\varepsilon_{2jn} = \frac{1}{E_n}[\sigma_{2jn} - \nu(\sigma_{1jn} + \sigma_{3jn})] - \varepsilon_{nl} \\ \varepsilon_{3jn} = \frac{1}{E_n}[\sigma_{3jn} - \nu(\sigma_{1jn} + \sigma_{2jn})] - \varepsilon_{nl} \end{cases} \tag{5}$$

$$\begin{cases}\varepsilon_{2jd} = \frac{1}{E_d}[\sigma_{2jd} - \nu(\sigma_{1jd} + \sigma_{3jd})] - \varepsilon_{dl} \\ \varepsilon_{3jd} = \frac{1}{E_d}[\sigma_{3jd} - \nu(\sigma_{1jd} + \sigma_{2jd})] - \varepsilon_{dl} \end{cases} \tag{6}$$

After gas adsorption, the relationship between the sorption strain of the bulk volume and the gas pressure can be given in a Langmuir type [26]. Assuming that coal is an isotropic medium, the horizontal sorption strains for normal coal and deformed coal can be described as:

$$\begin{cases}\varepsilon_{nl} = \frac{1}{3}\frac{\varepsilon_n^{\max} p}{p + p_n} \\ \varepsilon_{dl} = \frac{1}{3}\frac{\varepsilon_d^{\max} p}{p + p_d} \end{cases} \tag{7}$$

Solving Eq. (2), Eq. (3), Eq. (4), Eq. (5), Eq. (6) and Eq. (7), we can obtain the expressions of the additional interfacial stresses as follows:

$$\begin{cases}\Delta_2 = m_1(\sigma_1 - p) + m_3(\sigma_2 - p) + m_2(\sigma_3 - p) + m_4 \\ \Delta_3 = m_1(\sigma_1 - p) + m_2(\sigma_2 - p) + m_3(\sigma_3 - p) + m_4 \end{cases} \tag{8}$$

$$\begin{cases} m_1 = \frac{E_d\upsilon_n - E_n\upsilon_d}{E_n(1-\upsilon_d) + E_d(1-\upsilon_n)} \\ m_2 = \frac{2E_nE_d(\upsilon_n - \upsilon_d)}{(E_n + E_d)^2 - (E_n\upsilon_d + E_d\upsilon_n)^2} \\ m_3 = \frac{E_n^2(1-\upsilon_d^2) - E_d^2(1-\upsilon_n^2)}{(E_n + E_d)^2 - (E_n\upsilon_d + E_d\upsilon_n)^2} \\ m_4 = \frac{1}{3}\frac{E_dE_n}{E_n(1-\upsilon_d) + E_d(1-\upsilon_n)}\left(\frac{\varepsilon_n^{\max} p}{p + p_n} - \frac{\varepsilon_d^{\max} p}{p + p_d}\right) \end{cases} \tag{9}$$

According to Eq. (8), the factors that affect the additional interfacial stresses include the external stresses, internal gas pressure, gas sorption-induced swelling deformation and mechanical parameters of coal. Although the above results are based on the situation illustrated in Fig. 2 (a), they are the same as the results based on the other two situations.

3. Mechanical failure mechanisms and forms under ideal conditions

3.1. Failure criterion

The Mohr-Coulomb criterion can provide a good description of the failure of rock or coal. Its form is concise, and the parameters of this criterion have definite physical meanings. Accordingly, the Mohr-Coulomb criterion was widely used in the past. Therefore, this criterion was chosen as the failure criterion for the combination containing gas in this paper. The mechanical properties of coal can be affected by free gas and absorbed gas; however, we only consider the effect of free gas in this paper similar to the approach in the literature [27]. Assuming that the horizontal stress in the direction of level 3 is the minimum principal stress, in conjunction with Eq. (1), the equations for the Mohr-Coulomb criterion of the coal bodies far away from the interfaces are given as follows:

$$\begin{cases}(\sigma_1 - p) = \frac{1+\sin\varphi_n}{1-\sin\varphi_n}(\sigma_3 - p) + 2C_n\sqrt{\frac{1+\sin\varphi_n}{1-\sin\varphi_n}} \\ (\sigma_1 - p) = \frac{1+\sin\varphi_d}{1-\sin\varphi_d}(\sigma_3 - p) + 2C_d\sqrt{\frac{1+\sin\varphi_d}{1-\sin\varphi_d}} \end{cases} \tag{10}$$

The additional interfacial stresses make the effective horizontal stresses of the coal interfaces differ from those of the coal bodies. Considering Eq. (2) and Eq. (3), the equations for the Mohr-Coulomb criterion of the coal interfaces can be expressed as:

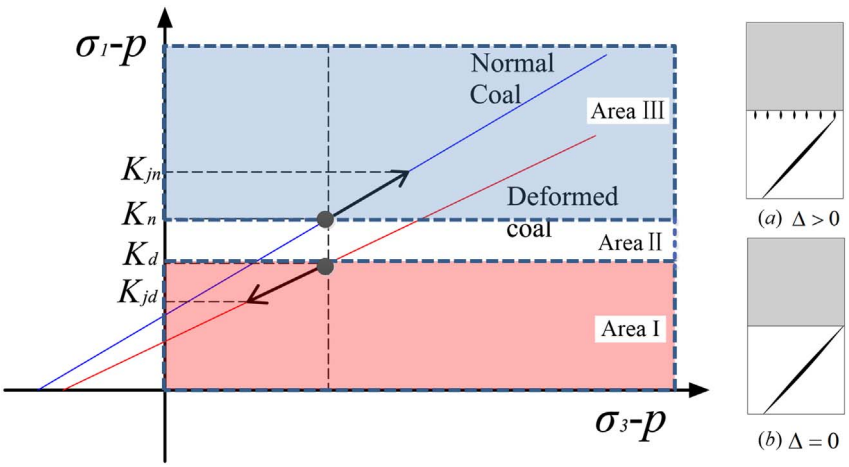

Fig. 3. Failure mechanisms and forms of coal-coal combination ($\Delta \geq 0$).

$$\begin{cases} (\sigma_1 - p) = \frac{1+\sin\varphi_n}{1-\sin\varphi_n}(\sigma_3 - p + \Delta_3) + 2C_n\sqrt{\frac{1+\sin\varphi_n}{1-\sin\varphi_n}} \\ (\sigma_1 - p) = \frac{1+\sin\varphi_d}{1-\sin\varphi_d}(\sigma_3 - p - \Delta_3) + 2C_d\sqrt{\frac{1+\sin\varphi_d}{1-\sin\varphi_d}} \end{cases} \tag{11}$$

Comparing Eq. (10) with Eq. (11), we can find that the additional interfacial stresses affect the effective compressive strengths of the coal interfaces mainly by changing their effective horizontal stresses. The failure of a coal body far away from an interface is controlled by the external stresses and internal gas pressure. However, the failure of a coal interface is controlled by a combination of the external stresses, internal gas pressure, gas sorption-induced swelling deformation and mechanical parameters of coal. Thus, the failure behaviors of coal interfaces are very complex.

3.2. Failure mechanisms and modes

As is well known, the additional interfacial stresses caused by uncoordinated horizontal deformation make the failure behaviors of the coal interfaces very complex. To better understand the damage behavior of coal combinations, uncoordinated deformation is described as the difference in the horizontal deformations between normal coal and deformed coal in the direction of the minimum principal stress. Then, uncoordinated deformation can be expressed as:

$$\Delta = \frac{[\sigma_3 - p - \upsilon_d(\sigma_1 - p + \sigma_2 - p)]}{E_d} - \frac{[\sigma_3 - p - \upsilon_n(\sigma_1 - p + \sigma_2 - p)]}{E_n} + \frac{1}{3}\left(\frac{\varepsilon_n^{\max} p}{p + p_n} - \frac{\varepsilon_d^{\max} p}{p + p_d}\right) \tag{12}$$

According to Fig. 3 and Eq. (12), we obtain the following rules. When the uncoordinated deformation is greater than zero ($\Delta > 0$), the normal coal interface is in compression, and the deformed coal interface is in tension, as shown in Fig. 2 (*a*). When $\Delta = 0$, there are no additional stresses at the interfaces, as shown in Fig. 2 (*b*). When $\Delta < 0$, the normal coal interface is in tension, and the deformed coal interface is in compression, as shown in Fig. 2 (*c*).

The compressive strengths of normal and deformed coal bodies are K_n and K_d, respectively, and the compressive strengths of normal and deformed coal interfaces are K_{jn} and K_{jd}, respectively. We have found that the additional interfacial stresses, which change the effective horizontal stress along the coal interface, lead to the difference between the compressive strengths of the coal body and coal interface. Therefore, the compressive strength of the coal interface is equal to the compressive strengths of the coal body under the same effective horizontal stresses. When the coal interface is in compression, the value of the compressive strength of the coal interface will move to the right along the failure envelope and become greater than the compressive strength of the coal body. When the coal interface is in tension, the value of the compressive strength of the coal interface will move to the left along the failure envelope and become less than the compressive strength of the coal body.

Two assumptions must be made before we analyze the mechanical failure mechanisms of the combination. First, the normal coal and deformed coal are both homogeneous media without any local defects. Second, the failure forms of coal are mainly shear and tension. As is universally well known, the strength of normal coal is greater than that of deformed coal, i.e., $K_n > K_d$. The strength of normal coal (K_n) and the strength of deformed coal (K_d) are defined as the demarcation points of the mechanical strength state. Then, the whole strength state can be divided into three areas: Area I ($\sigma_1 - p < K_d$), Area II ($K_d \leq \sigma_1 - p \leq K_n$) and Area III ($\sigma_1 - p \geq K_n$), as shown in Fig. 3 and Fig. 4.

When $\Delta > 0$, the normal coal interface is in compression, and the deformed coal interface is in tension. The value of the compressive strength of the normal coal interface will move to the right along its failure envelope and will appear in Area III. Therefore, the value of the compressive strength of the normal coal interface is greater than that of a normal coal body ($K_{jn} > K_n$). Meanwhile, the value of the compressive strength of the deformed coal interface will move to the left along its failure envelope and will appear in

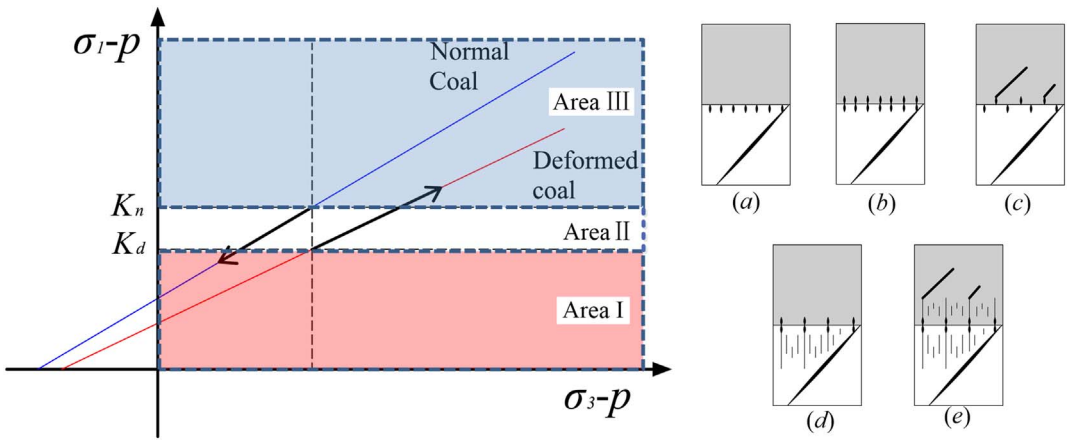

Fig. 4. Failure mechanisms and forms of coal-coal combination ($\Delta < 0$).

Area I. Therefore, the value of the compressive strength of the deformed coal interface is less than that of the deformed coal body ($K_{jd} < K_{\mathrm{d}}$). Finally, we can obtain this relationship between the strength values of the coal interfaces and coal bodies ($K_{jd} < K_{\mathrm{d}} < K_n < K_{jn}$), as the arrows demonstrate in Fig. 3. Depending upon this relationship, we can discover that splitting failure initially occurs along the deformed coal interface. Then, shear failure occurs within the deformed coal body. Finally, the failure of the normal and deformed coal combination will end with the complete destruction of the deformed coal, following which the further spread of damage into the normal coal body is difficult to achieve, as shown in Fig. 3 (*a*).

When $\Delta = 0$, there are no additional stresses at the interfaces. Therefore, the effective stress conditions of the coal bodies are the same as those of the coal interfaces. The relationship between the strength values of the coal interfaces and coal bodies is expressed as $K_{jd} = K_{\mathrm{d}} < K_n = K_{jn}$, as illustrated by the dots in Fig. 3. According to this relationship, shear failure initially occurs within the deformed coal and eventually leads to the complete destruction of the coal combination, as shown in Fig. 3 (*b*).

When $\Delta < 0$, the normal coal interface is in tension and the deformed coal interface is in compression. The value of the compressive strength along the normal coal interface will move to the left along its failure envelope, and it will appear in either Area II or Area I. Therefore, the value of the compressive strength of the normal coal interface is less than that of the normal coal body ($K_{jn} < K_n$). Additionally, the value of the compressive strength of the deformed coal interface will move to the right along its failure envelope and will appear in either Area II or Area III; therefore, it is greater than that of the deformed coal body ($K_{jd} > K_{\mathrm{d}}$). Combined with the aforementioned universal relationship ($K_n > K_{\mathrm{d}}$), the failure forms of normal and deformed coal combinations can be divided into five situations.

(a) When K_{jn} and K_{jd} both occur in Area II and when $K_{jd} < K_{jn}$, this relationship ($K_{\mathrm{d}} < K_{jd} < K_{jn} < K_n$) can be obtained. Shear failure initially occurs within the deformed coal body. Then, failure occurs at the deformed coal interface, for which the failure forms are mainly vertical cracking and powdering induced by faulting and rubbing. Finally, the failure of the coal combination will end with the complete destruction of the deformed coal, with little damage to the normal coal, as shown in Fig. 4 (*a*).

(b) When K_{jn} and K_{jd} both occur in Area II and when $K_{jn} < K_{jd}$, this relationship ($K_{\mathrm{d}} < K_{jn} < K_{jd} < K_n$) can be obtained. Shear failure initially occurs within the deformed coal body. Then, splitting failure first occurs at the normal coal interface. With the development of shear and splitting failure, the damage spreads further into the deformed coal interface, for which the failure forms are mainly vertical cracking and powdering. Finally, the failure of the coal will end with the complete destruction of the deformed coal, with some damage at the normal coal interface, as shown in Fig. 4 (*b*).

(c) When K_{jn} occurs in Area II and when K_{jd} is in Area III, this relationship ($K_{\mathrm{d}} < K_{jn} < K_n < K_{jd}$) can be obtained. Shear failure initially occurs within the deformed coal body. Then, splitting failure occurs at the normal coal interface. Subsequently, the damage spreads further into the normal coal body. With the development of failure, splitting failure occurs at the deformed coal interface, and the damage exists throughout the entire coal combination, as shown in Fig. 4 (*c*).

(d) When K_{jn} occurs in Area I and when K_{jd} is in Area II, this relationship ($K_{jn} < K_{\mathrm{d}} < K_{jd} < K_n$) can be obtained. Splitting failure initially occurs at the normal coal interface. Then, shear failure occurs within the deformed coal body. Furthermore, splitting failure occurs along the deformed coal interface. With the development of failure, the restrictions imposed upon the horizontal deformation, and the additional interfacial stresses will decrease, after which it is difficult to further spread the damage into the normal coal body. Therefore, there is substantial damage within the deformed coal and only some damage along the normal coal interface, as shown in Fig. 4 (*d*).

(e) When K_{jn} occurs in Area I and when K_{jd} is in Area III, this relationship ($K_{jn} < K_{\mathrm{d}} < K_n < K_{jd}$) can be obtained. Failure initially occurs at the normal coal interface. To remove restrictions imposed upon the horizontal deformation, the failure form is mainly represented by vertical splitting. Then, shear failure occurs within the deformed coal body. Subsequently, the destruction spreads further into the normal coal body. The above failure will make the additional interfacial stresses and K_{jd} smaller. The vertical splitting will spread from the normal coal interface into the deformed coal interface. Therefore, the damage exists throughout the entire coal combination, as shown in Fig. 4 (*e*).

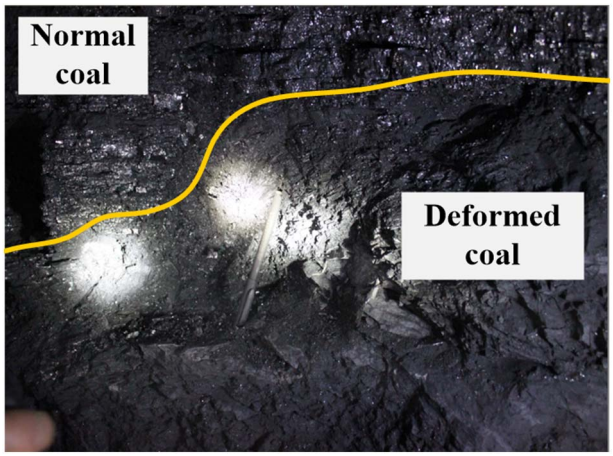

Fig. 5. The field distribution of normal coal and deformed coal.

In conclusion, there are seven failure forms for the normal and deformed coal combination containing gas. In most cases, failure occurs within the deformed coal. The local failure or whole failure of the normal coal will occur under some of the conditions. However, damage will exist within the normal coal under the condition that the deformed coal has been damaged. It is worth noting that these conclusions are obtained by ignoring local defects. If local defects are considered, the restrictions on the horizontal deformation between interfaces will be relieved, which makes the occurrence of failure within the deformed coal much more probable.

4. Discussion

4.1. Basic parameters of normal coal and deformed coal

The field distribution of normal coal and deformed coal from the Daning coal mine in China is presented in Fig. 5. The thickness of the entire coal seam is 4.73 m. There is a deformed coal layer with a thickness of 0.2 to 0.5 m in the middle to lower part of the coal seam, while all of the other layers are normal coal. The mechanical properties and adsorption constants of the coal samples were obtained by our experiments, as shown in Table 1. It is worth noting that the mechanical properties were all obtained under the condition of coal samples that do not contain gas.

According to Table 1, the mechanical properties of the normal coal are all greater than those of the deformed coal, except Poisson's ratio. Normal coal boasts a Young's modulus that is 14.2 times greater than that of deformed coal, and the uniaxial compressive strength of normal coal is 11.8 times greater than that of deformed coal. The cohesion and inner friction angle of normal coal are 8.6 and 1.4 times greater than those of deformed coal, respectively.

4.2. Failure mechanisms of coal combinations due to mining

In many cases, prior to the mining process, coal is not damaged by the natural stress field. Coal mining and roadway tunneling will induce a redistribution of stress, which may cause a failure of the coal. The Mohr circles for stress states under different stress paths induced by mining are presented in Fig. 6 (*a*). There are two primary paths of stress induced by mining. One path, which leads to a concentration of stress, is represented by horizontal stresses that essentially remain the same, while the vertical stresses increase. In this case, the radius of the Mohr circle for the stress states will increase, and the center of the Mohr circle will move to the right. Therefore, this situation will place the Mohr circle closer to the failure envelope, as shown in Fig. 6 (*b*). This stress path can be simulated by a complete stress-strain experiment with an unchanging confining stress in the laboratory. Accordingly, using the

Table 1
Basic parameters of the normal coal and deformed coal.

Parameters	Normal coal	Deformed coal
Young's modulus (MPa)	4054	286
Poisson's ratio	0.26	0.35
Cohesion (MPa)	3.79	0.44
Inner friction angle (°)	47	34
Uniaxial compressive strength (MPa)	19.58	1.66
Maximum sorption-induced strain	0.011	0.017
Sorption strain constant (MPa)	5.14	1.00

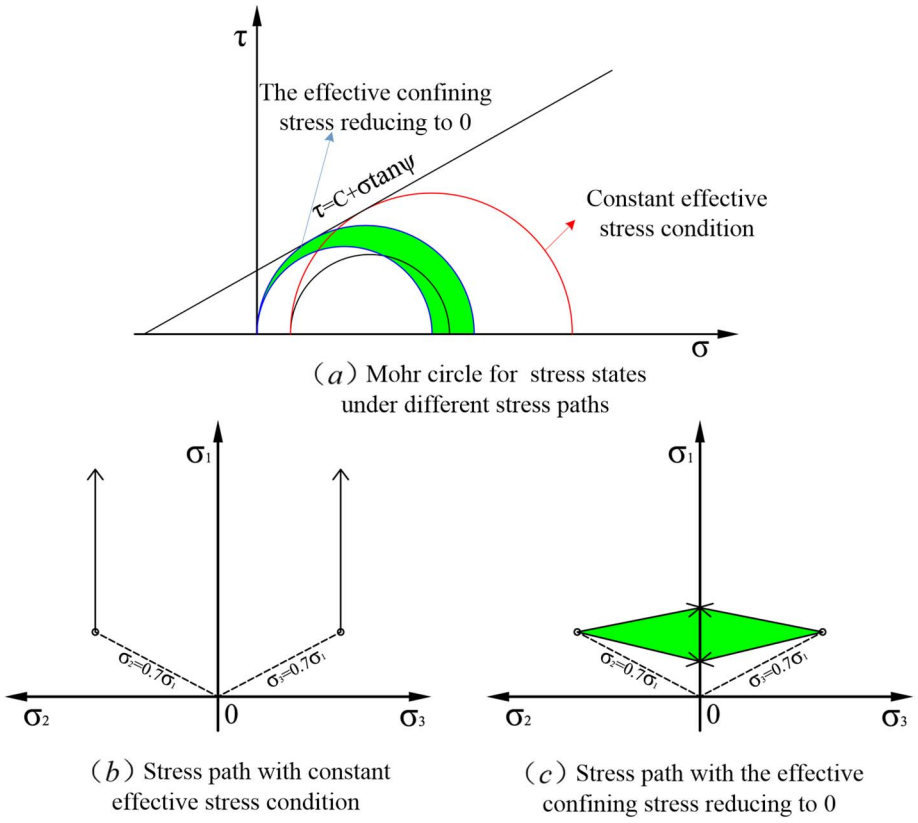

Fig. 6. Stress paths and failure of the coal-coal combination due to mining. (For interpretation of the references to color in this figure, the reader is referred to the web version of this article.)

corresponding experimental data, Wang et al. [27] analyzed the mechanical failure of coal induced by such a stress concentration. The other stress path is represented by a decrease of the horizontal stresses to zero, while the variation of the vertical stresses is small. The vertical stresses after mining may become slightly smaller or greater than the original stresses; thus, the green areas in Fig. 6 (b) and (c) indicate the ranges of the vertical stresses. In this case, the center of the Mohr circle for the stress states will move to the left, and the variation of the radius of the Mohr circle is small. Therefore, this situation will also place the Mohr circle closer to the failure envelope, as shown in Fig. 6 (*c*).

To conduct a quantitative analysis of the failure of the coal combination within the coal mine field, we presume that the depth of the coal combination is 500 m and that the average density of the overlying strata is 2500 kg/m^3. Then, we can deduce that the vertical stress of the coal combination is 12.5 MPa. In the Qinshui Basin, the ratio between the horizontal and vertical stresses is 0.7 [28], so the horizontal stress is 8.75 MPa. If the stress concentration factor ranges from 1.5 to 3, the vertical stress due to mining will reach 18.75 to 37.5 MPa.

For the first stress path, the horizontal stresses (8.75 MPa) are unchanged, while the vertical stress increases. If the gas pressure is assumed to be 1 MPa, all of the parameters are substituted into Eq. (10) and Eq. (11). Then, we calculate the effective compressive strengths of the normal and deformed coal bodies as 71.27 MP and 29.10 MPa, respectively. Because of the complexity of Eq. (11), the effective compressive strengths of the normal and deformed coal interfaces cannot be directly calculated; thus, we employ the graphic method to solve them. As shown in Fig. 7, when the line for the effective compressive strength of the coal body or interface intersects the line for the horizontal values that equals the ordinate values (HEO), the effective vertical stress ($\sigma_1 - p$) has reached the ultimate compressive strength of the coal body or interface.

According to Eq. (8), the additional interfacial stress is still affected by the effective vertical stress, even if the effective horizontal stress and gas pressure are unchanged. As shown in Fig. 7, when the effective vertical stress is lower than 12.04 MPa, the effective compressive strength of the normal coal interface in compression is greater than that of the normal coal body, and the effective compressive strength of the deformed coal interface in tension is lower than that of the deformed coal body. When the effective vertical stress is equal to 12.04 MPa, the effective compressive strength of the coal interface in compression is also equal to that of its body. When the effective vertical stress is greater than 12.04 MPa, the effective compressive strength of the normal coal interface in tension is lower than that of the normal coal body, and the compressive strength of the deformed coal interface in compression is greater than that of the deformed coal body.

According to Fig. 7, the line for the effective strength of the normal coal interface first intersects the HEO line at a value of 27.56 MPa. Then, the line for the effective strength of the deformed coal body intersects the HEO line at a value of 29.10 MPa. In this

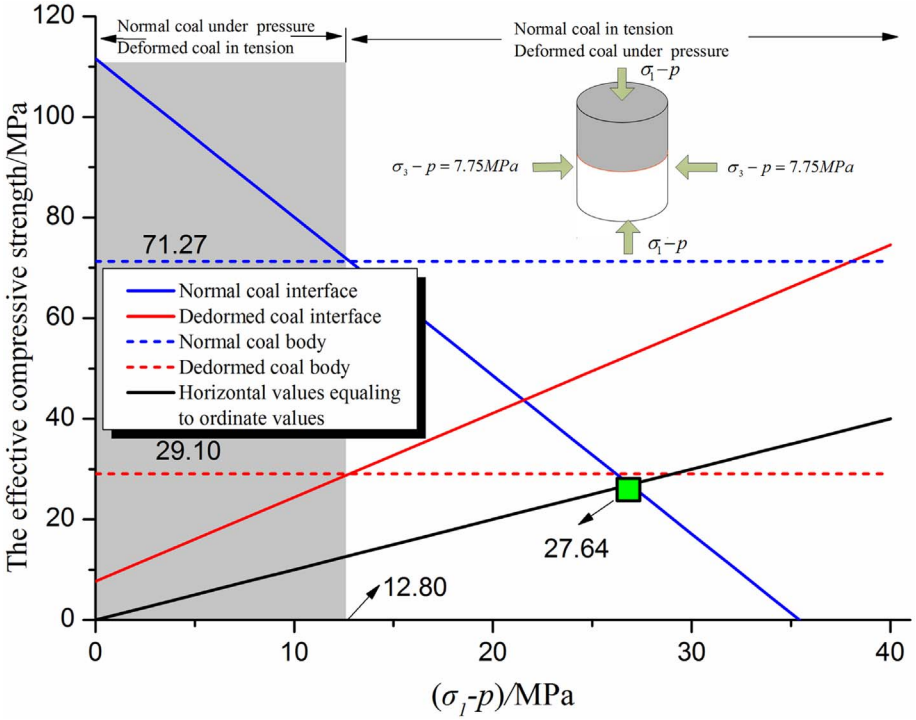

Fig. 7. Failure of the combination with an effective horizontal stress of 7.75 MPa.

case, failure first occurs within the normal coal interface, followed by the deformed coal body, and finally the normal coal body and deformed coal interface, as illustrated in Fig. 4 (*e*). For this stress path, when the effective vertical stress is at a lower level, the coal combination will not be destroyed. If the normal coal interface and deformed coal body are to be damaged, the stress concentration factors must reach 2.2 and 2.3, respectively. The stress concentration factor required to damage the normal coal body must reach 5.7, which is far greater than the range of the stress concentration factors with values of 1.5–3. Therefore, it is virtually impossible to damage the normal coal body. In this stress path, it is very difficult to destroy the coal combination, even if there is damage that is limited to the normal coal interface and deformed coal body.

For the second stress path, we assume that the horizontal stress is directly reduced to zero and that the gas pressure is also zero. Then, substituting all of the parameters into Eq. (10) and Eq. (11), we can obtain the uniaxial compressive strengths of the normal

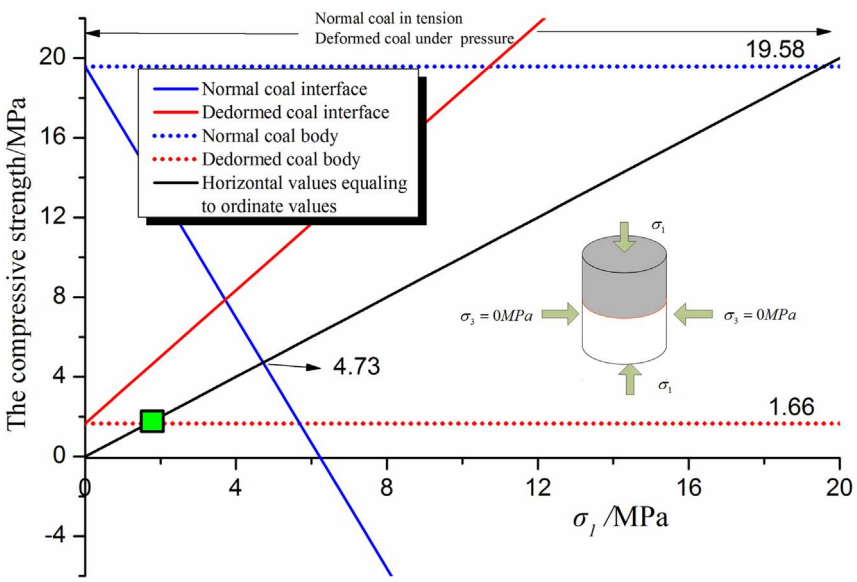

Fig. 8. Failure of the combination with an effective horizontal stress of 0 MPa.

and deformed coal bodies, at 19.58 MP and 1.66 MPa, respectively. We also employ the graphic method for obtaining the effective compressive strengths of the normal and deformed coal interfaces, as shown in Fig. 8.

According to Fig. 8, the interfaces of the normal coal and deformed coal are in tension and compression, respectively, during the compression phase of the effective vertical stress. With an increase of the effective vertical stress, the effective strength of the normal coal interface will decrease from its uniaxial compressive strength of 19.58 MPa, and the effective strength of the deformed coal interface will increase from its uniaxial compressive strength of 1.66 MPa. First, the line for the effective strength of the deformed coal body intersects the HEO line at a value of 1.66 MPa. Then, the line for the effective strength of the normal coal interface intersects the HEO line at a value of 4.73 MPa. Finally, the line for the effective strength of the normal coal body intersects the HEO line at a value of 19.58 MPa. The failure form of the combination is shown in Fig. 4 (*c*). We discover that there is damage within the deformed coal body and along the normal coal interface without any stress concentration, wherein the stress concentration factor required to damage the normal coal body must reach 1.6, which can be achieved under certain conditions. Due to the additional constraint of deformed coal, the required value for the failure of the normal coal interface is much lower than that for the normal coal body, which suggests that the existence of deformed coal can promote the damage of the normal coal. In this stress path, failure is more likely to occur within the deformed coal body and along the normal coal interface, and the damage will spread further into the normal coal body under certain conditions.

In Fig. 7 and Fig. 8, when the effective vertical stress ($\sigma_1 - p$) is greater than zero, there is no intersection between the line of the effective strength of the deformed coal interface and the HEO line. The intersection of the two lines occurs in the area where the effective vertical stress is less than zero. However, if the gas pressure is greater than the vertical stress, the gas will diffuse from the coal until the gas pressure is equal to the vertical stress. Therefore, the effective vertical stress cannot be less than zero in real-life situations. If we calculate the effective strengths of the normal and deformed coal interfaces according to the method of [11] and subsequently use them to analyze the mechanical failure mechanisms of the combination, an erroneous result would be obtained due to neglecting the gas pressure, which must be less than or equal to the vertical stress. Thus, the best method for obtaining the effective compressive strengths of normal and deformed coal interfaces is the graphic method in our paper.

Compared with the two stress paths, we can observe that failure is more likely to occur within a deformed coal body and along a normal coal interface and that the existence of deformed coal can promote the destruction of a normal coal body. The combination in the second stress path is much more easily destroyed than that in the first stress path. The second stress path is usually induced by tunneling for coal near the working face, where there is a significant plastic zone. The first stress path is usually induced by mining for coal far away from the working face, where there is little plastic deformation.

The deformation of coal induced by tectonics provides favorable conditions for coal and gas outbursts, but the understanding of the failure mechanisms for the normal and deformed coal combination is still very limited. In this study, seven failure forms of a coal combination containing gas were observed, and the failure mechanisms of the combination due to mining were discussed. According to the results, we observed that especially in the first stress path, additional reinforcement measures and stress relief technologies should be applied within the deformed coal to prevent the failure of the coal combination.

5. Conclusions

The main conclusions are as follows:

1) Due to uncoordinated horizontal deformation, additional stresses exist along the interfaces of the normal and deformed coal combination that contains gas. The additional interfacial stress is affected by the external stresses, internal gas pressure, gas sorption-induced swelling deformation and mechanical parameters of coal. Furthermore, the additional stresses of the normal coal and deformed coal are equal and opposite.
2) The additional interfacial stresses make the failure behaviors of the coal interfaces very complex, and they affect the effective compressive strengths of the coal interfaces mainly by changing their effective horizontal stresses. The uncoordinated deformation is defined as the difference of the horizontal deformations between normal coal and deformed coal in the direction of the minimum principal stress. According to this uncoordinated deformation, seven failure forms of the normal and deformed coal combination containing gas are obtained. In most cases, the destruction of the combination is caused by the structural failure of the deformed coal.
3) There are two primary paths of stress that are induced by mining. One path is represented by horizontal stresses that essentially remain the same, while the vertical stress increases. The other stress path is represented by horizontal stresses that decrease to zero, while the variation of the vertical stress is small. The combination in the second stress path is much more easily damaged than that in the first stress path. Comparing the two stress paths, we observed that failure is more likely to occur within a deformed coal body and along a normal coal interface and that the existence of deformed coal can promote the destruction of normal coal.

These research results can help us to better understand the role of mechanical failure of combinations on coal and gas outbursts and provide a theoretical basis for the control of coal and gas outbursts.

Nomenclature

σ	stress (MPa)
p	gas pressure (MPa)
Δ	additional interfacial stress (MPa)
ε	strain (dimensionless)
E	Young's modulus (MPa)
ν	Poisson's ratio (dimensionless)
C	cohesion (MPa)
φ	inner friction angle (°)
K	effective compressive strength (MPa)
p_ε	Langmuir-type matrix sorption strain constant (MPa)
ε_l	horizontal sorption strain
ε^{max}	maximum sorption-induced strain of volume
m_1, m_2, m_3, m_4	coefficient

Subscripts and superscripts

n	normal coal
d	deformed coal
j	interface
1, 2, 3	coordinate axes

Acknowledgments

Financial support is provided by the Open Funds (WS2017B05) of State Key Laboratory Cultivation Base for Gas Geology and Gas Control (Henan Polytechnic University), the National Science Foundation of China (51574153, 51504140 and 51574229), the Natural Science Foundation of Shandong Province (ZR2014EEM043) and China Postdoctoral Fund (2016M602170 and 2017T100508).

References

[1] F.H. An, Y.P. Cheng, L. Wang, W. Li, A numerical model for outburst including the effect of adsorbed gas on coal deformation and mechanical properties, Comput. Geotech. 54 (2013) 222–231.
[2] W. Zhao, Y. Cheng, H. Jiang, K. Jin, H. Wang, L. Wang, Role of the rapid gas desorption of coal powders in the development stage of outbursts, J. Nat. Gas Sci. Eng. 28 (2016) 491–501.
[3] S. Kong, Y. Cheng, T. Ren, H. Liu, A sequential approach to control gas for the extraction of multi-gassy coal seams from traditional gas well drainage to mining-induced stress relief, Appl. Energy 131 (2014) 67–78.
[4] H. Li, Major and minor structural features of a bedding shear zone along a coal seam and related gas outburst, Pingdingshan coalfield, northern China, Int. J. Coal Geol. 47 (2001) 101–113.
[5] H. Li, Y. Ogawa, Pore structure of sheared coals and related coalbed methane, Environ. Geol. 40 (2001) 1455–1461.
[6] H. Li, Y. Ogawa, S. Shimada, Mechanism of methane flow through sheared coals and its role on methane recovery, Fuel 82 (2003) 1271–1279.
[7] B. Jiang, Z. Qu, G.G.X. Wang, M. Li, Effects of structural deformation on formation of coalbed methane reservoirs in Huaibei coalfield, China, Int. J. Coal Geol. 82 (2010) 175–183.
[8] W. Wang, Y.P. Cheng, H.F. Wang, H.Y. Liu, L. Wang, W. Li, et al., Fracture failure analysis of hard–thick sandstone roof and its controlling effect on gas emission in underground ultra-thick coal extraction, Eng. Fail. Anal. 54 (2015) 150–162.
[9] B. Jia, X.M. Ni, The critical gas pressure of coal and gas outburst with different coal structure combination, Coal Sci. Technol. 40 (2012) 69–72.
[10] P. Duffaut, Structural Weaknesses in Rocks and Rock Masses Tentative Classification and Behaviour, ISRM International Symposium, International Society for Rock Mechanics, 1981.
[11] G.P. Tziallas, H. Saroglou, G. Tsiambaos, Determination of mechanical properties of flysch using laboratory methods, Eng. Geol. 166 (2013) 81–89.
[12] X. Xian, X. Tan. Destroy Mechanism of Stratified Rocks.s Chongqing University Press, 1989.
[13] J. Li, Y. Wang, Analysis for failure modes and interfacial stress of rock mass with horizontal weak interlayer, Journal of Liaoning Technical University: Nat. Sci. 3 (2015) 710–715.
[14] L. Dou, C. Lu, Z. Mou, X. Zhang, Z. Li, Rock burst tendency of coal rock combinations sample, J. Min. Saf. Eng. 23 (2006) 43–46.
[15] Z. Zhao, W. Wang, C. Dai, J. Yan, Failure characteristics of three-body model composed of rock and coal with different strength and stiffness, Trans. Nonferrous Metals Soc. China 24 (2014) 1538–1546.
[16] J. Zuo, H. Xie, A. Wu, J. Liu, Investigation on failure mechanisms and mechanical behaviors of deep coal-rock single body and combined body, Chin. J. Rock Mech. Eng. 30 (2011) 84–92.
[17] J. Liu, E. Wang, D. Song, S. Wang, Y. Niu, Effect of rock strength on failure mode and mechanical behavior of composite samples, Arab. J. Geosci. 7 (2015) 4527–4539.
[18] Z. Zhang, J. Liu, L. Wang, H. Yang, J. Zuo, Effects of combination mode on mechanical properties and failure characteristics of the coal-rock combinations, J. China Coal Soc. 37 (2012) 1677–1681.
[19] D. Guo, J. Zuo, Y. Zhang, R. Yang, Research on strength and failure mechanism of deep coal-rock combination bodies of different inclined angles, Rock Soil Mech. 32 (2011) 1333–1339.
[20] Z. Zhao, W. Wang, L. Wang, C. Dai, Compression-shear strength criterion of coal-rock combination model considering interface effect, Tunn. Undergr. Space Technol. 47 (2015) 193–199.
[21] Y. Li, Z. Tan, Numerical analysis for the relationship of tectonic-coal layer's horizon in coal and gas outburst, Safety in Coal Mines 42 (2011) 5–8.
[22] D. Duan, H. Wang, X. Feng, Q. Dong, Microseism precursory characteristics of coal and gas outburst for contains different thickness of soft stratification, Safety in Coal Mines 42 (2011) 9–11.

[23] S. Lu, Y. Cheng, J. Ma, Y. Zhang, Application of in-seam directional drilling technology for gas drainage with benefits to gas outburst control and greenhouse gas reductions in Daning coal mine, China, Nat. Hazards 73 (2014) 1419–1437.
[24] S.Q. Lu, Y.P. Cheng, W. Li, L. Wang, Pore structure and its impact on CH_4 adsorption capability and diffusion characteristics of normal and deformed coals from Qinshui Basin, Int. J. Oil Gas Coal Technol. 10 (2015) 76–78.
[25] L. Liu, W. Liang, Y. Li, F. Lu, W. Zhu, Influence of mechanical characteristic of bedding surface on stratified composite rock mass, J. Min. Saf. Eng. 23 (2006) 187–191.
[26] J.R. Levine, Model Study of the Influence of Matrix Shrinkage on Absolute Permeability of Coal Bed Reservoirs, 109 Geological Society, London, Special Publications, 1996, pp. 197–212.
[27] S. Wang, D. Elsworth, J. Liu, Permeability evolution during progressive deformation of intact coal and implications for instability in underground coal seams, Int. J. Rock Mech. Min. Sci. 58 (2013) 34–45.
[28] Z. Meng, J. Zhang, R. Wang, In-situ stress, pore pressure and stress-dependent permeability in the Southern Qinshui Basin, Int. J. Rock Mech. Min. Sci. 48 (2011) 122–131.